Spectrochimica Acta Part A: Molecular and Biomolecular Spectroscopy 212 (2019) 155–159

Contents lists available at ScienceDirect

Spectrochimica Acta Part A: Molecular and Biomolecular Spectroscopy

journal homepage: www.elsevier.com/locate/saa

Non-invasive monitoring of red beet development

Bing Ma, Raul D. Rodriguez *, Elena Bogatova, Alexey Ruban, Sergey Turanov, Damir Valiev, Evgeniya Sheremet *

Tomsk Polytechnic University, Lenina ave. 30, 634034 Tomsk, Russia

ARTICLE INFO

Article history:
Received 30 October 2018
Received in revised form 19 December 2018
Accepted 1 January 2019
Available online 04 January 2019

Keywords:
Red beets
Betalain
Raman spectroscopy
Plant chemistry
Plant aging
Agriculture
Artificial lightning
Greenhouse

ABSTRACT

Agricultural monitoring is required to enhance crop production, control plant stress, and predict pests and crop infection. Apart from monitoring the external influences, the state of the plant itself must be tracked. However, the modern methods for plant analysis are expensive and require plants processing often in a destructive way. Optical spectroscopy can be used for the non-invasive monitoring requiring no consumables, and little to none sample preparation. In this context, we found that the red beet growth can be monitored by Raman spectroscopy. Our analysis shows that, as plants age, the rate of betalain content increases. This increase makes betalain dominate the whole Raman spectra over other plant components. The dominance of betalain facilitates its use as a molecular marker for plant growth. This finding has implications in the understanding of plant physiology, particularly important for greenhouse growth and the optimization of external conditions such as artificial illumination.

1. Introduction

Food production and food security are at the topmost list of critical issues affecting the non-stopping growing of human population. Modern agriculture is strongly influenced by technology to improve efficiency and make it more sustainable. By putting together information from sensors, satellites, and soil sampling, farmers can significantly reduce the use of material and human resources and pesticides. The increase in farming performance has strong environmental and economic implications. However, complex systems for highly-performance farming lack a cost-efficient and objective method to monitor plant growth [1].

Generally speaking, the fruit ripening and leaf senescence are governed by external (nutrient availability, draught, and other stressors) and internal factors (plant age) [2]. While the fruit ripening is visible by the color change due to the increase in carotenoid content, an earlier sign is the change of glucose level, this is observed in many vegetables and fruits [3,4]. Carotenoids contents also decrease on infection sites [5]. Similarly, the leaf senescence is manifested first by protein degradation, further by the change of color, and only then after it is followed by DNA damage [6]. By catching the early changes in the state of the plant, a farmer could take measures to enhance or recover crops growth.

Most techniques for biochemical plant analysis are based on chromatographic methods [7,8]. This method of separating the mixture into components is based on distinguishing their physical and chemical properties. One of these methods is solid-phase microextraction (SPME) that is a successful solvent-free sampling technique. The advantage of the method is the absence of the use of solvents for the extraction of analytes from absorption coatings [9]. But SPME typically requires collecting the samples from the field, extensive sample preparation, and costly consumables. While suitable for laboratory studies, it is not a cost-efficient tool of precision agriculture. Optical methods like infrared spectroscopy (IR) [10,11] and Raman spectroscopy, on the contrary, offer consumable-free and specific and quantitative chemical analysis [12]. While Raman spectroscopy involves the excitation of a molecule by inelastic scattering with a photon (from a laser light source), infrared spectroscopy detects the absorption of photons, with the molecule being excited to a higher vibrational energy level [13]. The spread of Raman spectroscopy is highly aided by the development of chemometric software and portable Raman spectrometer devices that nowadays can fit on the palm of our hands [14–16].

In most cases, optical measurements can be carried out directly on plant tissues in the field eliminating complications involved with lengthy and cumbersome sample preparation requirements. The vibrational bands from the measured sample provide information about the chemical composition, including both primary and secondary metabolites. Also, based on such markers related to individual plant substances, spectroscopic analyses in principle allow the discrimination of different types of chemotypes and even distinguishing among the same species.

* Corresponding authors.
E-mail addresses: rodriguez@tpu.ru (R.D. Rodriguez), esheremet@tpu.ru (E. Sheremet)

https://doi.org/10.1016/j.saa.2019.01.006
1386-1425/

With the development of Raman spectroscopy, this method has become widely used and has the advantage to determine the composition of the substance [17]. Raman spectroscopy is most sensitive to carotenoid content and is widely and successfully used for the structural and compound analysis of various plants, vegetables, and fruits [5]. The use of Raman scattering of light on plants began with the study of cellulose [18] and the skeletal component of plants [19]. Over the last decade, the possibility of Raman spectroscopy as a non-destructive method was demonstrated on several cellulose fibers, for example, flax, cotton [20], jute, ramie, Kapok, sisal, and coconut fibers [21]. An assessment of the presence of cellulose in apples and comparison of structural differences of cellulose of different origin was successfully carried out [22]. The classification of various vegetable oils and the quantitative evaluation of olive oil falsification by Raman spectroscopy were also performed by several groups [23]. In this work, the red beet was selected for the demonstration of the method potential for several reasons: the monitoring of the leaf state would give insights in the development of the root that is much harder to access by others methods. Microelements in the red beet promote healthy hematopoiesis, increase iodine level in the body ensuring the health of the thyroid gland. Folic acid helps to form the nervous system of the fetus in pregnant women [24]. Moreover, the red beet pigment, betalain, is an important lipotropic substance that regulates fat metabolism, prevents liver infiltration, and decreases blood pressure. Another reason for the study of the beet is its economic significance. In some emerging economies, like in Russia, red beet makes an important economic impact since it is used as a sugar precursor. Since the year 2000, a program has been underway to increase sugar beet production to reduce dependence on sugar imports [25].

Beetroots are used in food production, but it is also possible to consume leaves since they show up to five times higher oxygen radical absorbance capacity (ORAC) values than the roots [26]. Leaves and roots are rich in phenolic compounds and flavonoids, whose concentration is rising to the 55-60th day of growth while the old leaves tend to accumulate oxalates [26]. Their concentrations have been shown to be influenced by the growth conditions [27]. Besides beetroots, betalains were also found in different quinoa grains in a previous study using chromatography [28]. Also, the amount of macro- and micronutrients or toxins in red beet, as in any other plant, depends on the growth conditions, including illumination, namely on the spectral characteristics of the illumination and its intensity [29]. Motivated by its antioxidant properties, a previous report showed the increase of total betalain content in hairy roots of red beet with age [30]. The amount increased from 6th to 15th day and reached its maximum at 15th day. However, the sugar composition in the growth medium affects not only the root morphology but also suppresses the betalain synthesis [31]. Other reasons can affect the content of betalain; water stress leads to betalain and phenolics accumulation in the roots [32] while increasing fiber contents in all the parts of the plant [33]. The fiber accumulation was also observed under severe light reduction [32]. All these works illustrate the relevance of being able to track the changes that occur in the plant chemistry over time, and this is the exact question we want to investigate for the case of red beet using Raman spectroscopy.

2. Experimental

2.1. Red Beet Samples

The red beet cultivar “Bona” was chosen as a model plant. The plants were purchased from Sortsemovoshch, St. Petersburg, Russia. Experimental samples of red beet were previously sprouted for two days before the seedling emergence. The samples were evenly separated into pots (7 seeds per pot). The pots were placed in cells with a microclimate and irradiation control – phytotrons (Fig. 1ab). Throughout the experiment, the temperature of 23 ± 2 °C and humidity 70% were kept constant in all cells. The plants were watered manually every day with 300 ml of distilled water for each pot.

The operating modes of irradiation were selected in such a way that the total flux of light in the region of photosynthetically active radiation (PAR) was the same in all cells of phytotrons (Table 1S), but at the same time made different spectral quality (Fig. 1c). The photoperiod was fixed to 16 h. The adjustment of illumination modes was carried out by changing the light-emitting diodes (LED) current. This was the most convenient and easily controlled method for controlling the intensity of the LED's radiation, that was the selection of the radiation spectrum of the entire facility. The parameters of the irradiation facility, given in Table 1S and Fig. 1c, were measured using a “TKA-Spectrum” (PAR) spectrophotometer (TKA Scientific instruments Russia).

2.2. Raman Experiment

The red beet stems were fixed on glass slides by double-sided tape. The Raman spectroscopy experiments were performed with a DXR2Xi Raman Imaging Microscope from Thermo Fisher Scientific U.S.A. We found that using a tightly-focused laser beam (785 nm, 10× objective and N.A. 0.25), we could obtain spectra with a good signal/noise ratio, 1 s exposure time, 15 repetitions, and 10 mW power at the sample. When using a confocal microscopy setup, the probed volume is limited by the optics to a few micrometers, and thus the substrate's signal does not need to be considered. For every cell, two stems were selected for the Raman measurements. For older red beet stems, two points were measured on each stem. For younger red beet samples, due to lower

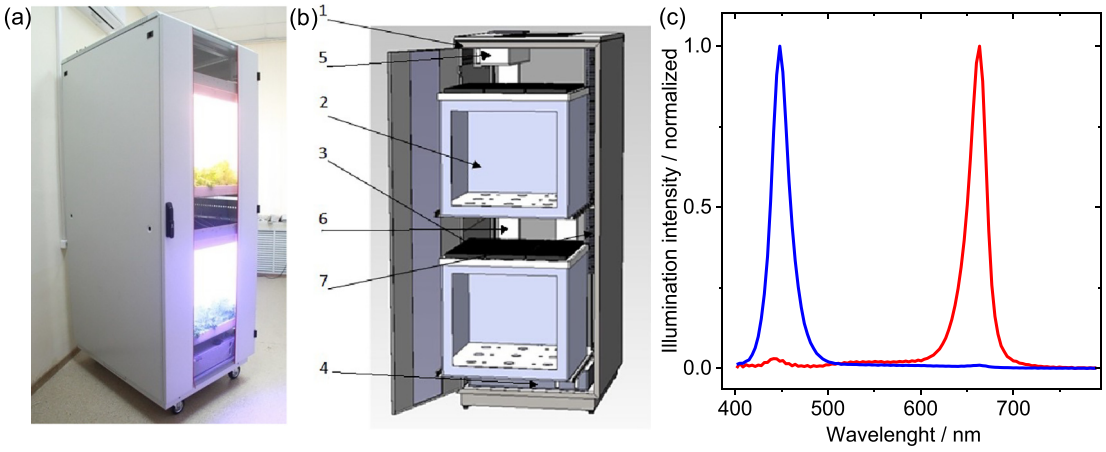

Fig. 1. (a) Picture of the “Phytotron” greenhouse used to grow the beets (b) Phytotron greenhouse layout: 1 - the frame, 2 - phytotron cells, 3 - lamps with independent regulation of the plant irradiation, 4, 5 - irrigation system (lower and upper tanks), 6 - microclimate system, 7 - electrical power and control system. (c) Illumination spectra of the two different cells used.

signal intensity for younger red beets (see Fig. 3ac), three points were chosen on each stem to get accurately averaged spectra. For this case, we used 2 s exposure time, 15 repetitions, and 10 mW laser power at the sample. Therefore, for each cell, we obtained 4 spectra of older stems and 6 spectra of younger stems. Afterward, the fluorescence background subtraction and spectra intensity normalization were performed with respect to the peak at 1394 cm^{-1}. Then the normalized spectra from four measured points of old stems and six spectra from six measured points of young stems were averaged separately. We also analyzed all individual spectra manually (before average) since some statistical information could be lost by averaging. We found that although there are spectral variations in the components, it is the intensity ratio of betalain to carotene that remains a robust indicator from sample to sample and from one harvest to another. Different averaged spectra like spectra of older and younger stems, spectra of the cells 1 and 2 were plotted together to compare them.

3. Results and Discussion

3.1. Analysis of the Raman Spectra of Leaves and Stems

Fig. 2 shows the spectra of stem and leaves. An intense purple color characterizes the stems, while the leaves have red and green shades as can be seen from the pictures in Fig. 2.

The most intense feature in the Raman spectrum of the green leaf appears at 1527 cm^{-1}. It typically appears for conjugated polyene chain (—C═C—) in carotenoids [32,34]. The C—C and C—N and stretching modes of carotenoids appear at 1187 and 1158 cm^{-1}, and 1004 cm^{-1} mode is attributed to CH_3 in-plane rocking mode. Chlorophyll also shows the bands at 1553, 1287, 989 and 919 cm^{-1} that are assigned in Table 1. The Raman spectra of the stem are dominated by

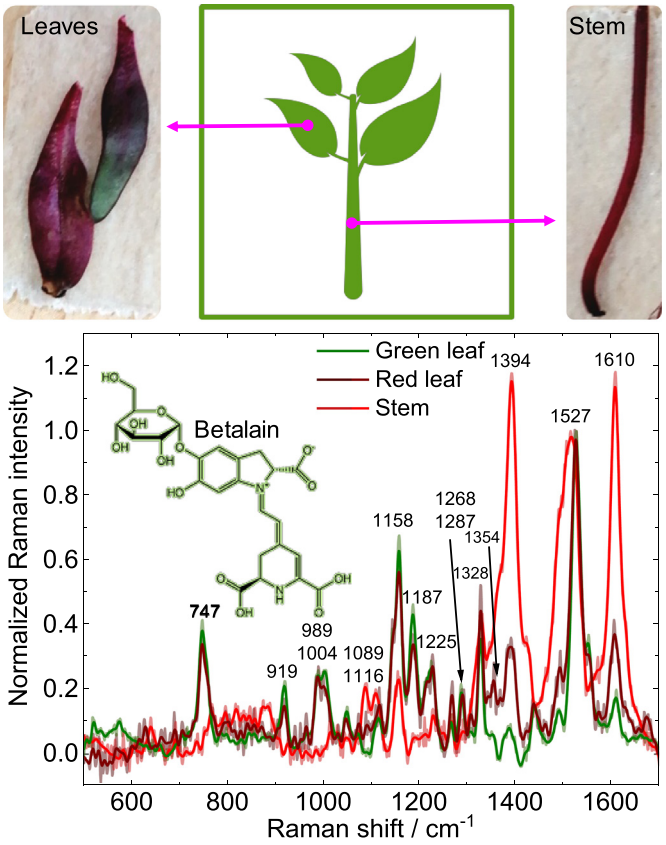

Fig. 2. Top: photographs from the different parts of red beet investigated in this work. Bottom: Raman spectra of leaves and stems with the main peak positions labeled, and the molecular structure of betalain presented as an inset.

Table 1
Raman bands observed in the spectra (in cm^{-1}) and their assignments for red beet leaves and stems.

Green leaf	Red leaf	43-Day stem	13-Day stem	Assignment
1610	1607	1610	1610	$^{13}C═^{12}C$
1553	1554	–	–	Chlorophyll ν(pyrimidine ring) + $\delta(CH_3)$
1527	1526	1524	1524	Carotenoid —C═C—
1486	1492	–	–	$\delta(CH_3)$
1438	1438	–	–	CH_3/CH_2 bend
1391	1389	1394	1394	CH rocking
1354	1354	1349	1349	$\nu(C—NO_2)$
1328	1328	1330	1330	C—H, O—H
1287	1290	–	–	Chlorophyll ν(C—N) + $\rho(CH_3)$
1267	1268	–	–	═CH-rocking modes
1225	1228	1230	1230	N—H bending vibration and C—N stretching
1187	1189	–	–	Carotenoids C—C stretching mode
1158	1158	–	–	Protein (stretching C—C, C—N) carotenoid
1112	1116	–	–	Carbohydrates C—OH bending
–	–	1086, 1106	1086, 1106	$^{13}C═S$
1049	1046	1050	1050	C—O—H vibrations
1004	1002	–	–	Carotenoid in-plane CH_3 rocking
989	987	–	–	Chlorophyll
919	919	–	–	Chlorophyll
–	–	889	889	$\rho(CH_2)$ + ν(C—C)
–	–	–	764	Tryptophan
747	746	745	–	Asym C—S—C
576	570	–	–	Carbohydrates, δ (C—C—O) + τ(C—O)
532	532	532	532	C—O—C glycosidic link

the three peaks at 1394 cm^{-1}, 1524 cm^{-1} and 1610 cm^{-1} as well as weaker but pronounced modes at 1086, 1106, and 1158 cm^{-1}. The modes at 1387 (with a lower-frequency shoulder), 1517, 1603, and also weaker 562, 1014, 1115, 1157 and above 1800 cm^{-1} appear for purified betalain [35], the red-purple pigment in red beet, a water-soluble nitrogen-containing pigment (4-(2-oxoethylidene)-1,2,3,4-tetrahydropyridine-2,6-dicarboxylic acid). The molecular structure of betalain is depicted in the inset of Fig. 2 [36]. In the plant, betalain is found together with betaxanthin, a yellow or orange dye. The average amount of betalains is about 1% of solid weight [37]. Despite the relatively low concentration in plants, betalains exhibit a strong Raman signal due to high optical absorption. The literature still lacks a thorough interpretation of betalain spectra and the physical origin of the different vibrations experimentally observed. According to previous reports [38,39], the vibration at 1610 cm^{-1} is attributed to C═C and C═N stretching modes in the pyridine and indole rings. Based on DFT calculations [40], it was also predicted a vibrational mode at 1603 cm^{-1} attributed to two in-plane C—C stretching modes on the C10—C11═C12—C13═C14—C15 chain but their calculations do not include the assessment of Raman activity and thus cannot be directly applied to the spectral interpretation. The reported modes of isolated carotenes in red beet appear to be at 1523 and 1055 (C—C) and 1021/993 (C—CH_3) cm^{-1} [32,34,41]. The mode at 1394 cm^{-1} originates from the deformation of CH_3 bonds [42]. A range of less-specific bands is also visible in the spectra and is listed and assigned in Table 1. The spectra from red beet leaf appear to be a mixture of two components. We confirmed this by matching the assignment of the Raman bands to carotenoids and betalain. We also suggest that the double-feature at 1524 cm^{-1} is composed of two modes: the carotenoid feature at 1527 cm^{-1} and a betalain feature at 1517 cm^{-1}.

3.2. Raman Spectra of Growing Beet

In Fig. 3 we show the Raman spectra of red beet stems with different ages, 13 and 43 days old. Each spectrum in the left-hand side is an average of all the spectra taken on one stem. The data include the results for stems from cell 1 (top row) and cell 2 (bottom row). For easier

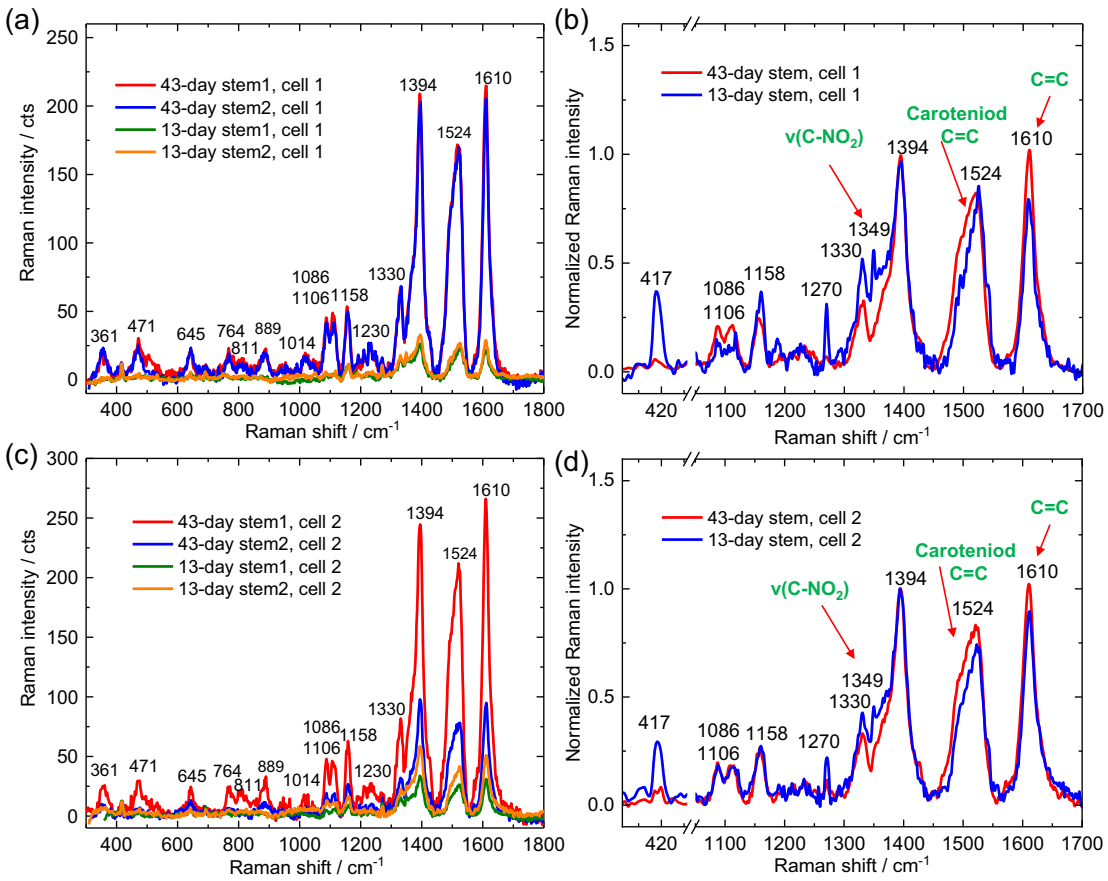

Fig. 3. Raman spectra of red beet stem. (a) Non-normalized cell 1. (b) Normalized cell 1. (c) Non-normalized cell 2. (d) Normalized cell 2.

comparison, the spectra in the right-hand side are the normalized spectra averaged for both measured stems. The obvious difference is the increase in the signal intensity with the plant's development. We also observed a significant change in the intensity ratios for the two peaks at 1517 cm^{-1} and 1523 cm^{-1}. Their ratio for the 43-day old plant was 1.00 and 0.96 for the cells 1 and 2; for the 13-day old stems, it was 0.87 and 0.89 respectively. Also, we found an increase in the 1610 cm^{-1} mode intensity observed for betalain as compared to carotene. To the best of our knowledge, most of the studies on red beet were performed on the roots while the question of pigment accumulation in leaves and stems was not investigated until now. The betalain accumulation also explains the apparent disappearance of some bands in the normalized spectra of the old beets stems as they get screened by the much larger signal from betalain.

The other observed peaks originate from the remaining plant components such as saccharides, amino acids, and probably essential oils. The unambiguous assignment is difficult because many modes would be covered by the intense pigment signal. In particular, we found that the intensity and FWHM of several peaks such as at 417, 1270, and 1349 cm^{-1} change with the increase in red beet age. Following previous literature reports, we found that the peak at 417 cm^{-1} accurately refers to the saccharides. Other peaks that change their intensity can be attributed to saccharides and amino acids [41]. For the older plants, the Raman signal/noise ratios were better than for the younger ones. We attribute this intensity difference to the betalain quantity increase in the stem. This increase in betalain concentration over time resulted in a Raman signal so intense that it even masked the signal from other components in the beet. Another possible explanation that sugar contents decrease with plant age would contradict the work by Austin [43] and is thus not considered further here. However, the data previously reported are not conclusive and thus in follow up works the investigation of red beet at different laser excitations will help elucidating changes in other plant components absorbing under a particular spectral range (in green or red that are common lasers in Raman investigations). This spectral matching is what gives rise to resonant Raman spectroscopy and could allow complementing the insights reported in this work.

4. Conclusion

Our work offers a novel way to investigate the dynamics of plants growth based on the Raman spectroscopy tracking of betalain. As red beets grow, the nutrients contents are constantly changing. But the growth rates are not the same for the different compounds inside the plant. We found that the accumulation rate of betalain is higher than that of any other component in the plant's stem. This fast increase rate makes the nutrients redistribute in the stem of red beet. This situation could introduce complications in the Raman analysis making it hard to see the signature of other components in the spectra obtained from older stems. Contrary to our expectations, we found that the illumination conditions possibly did not play the major role in the time-evolution of betalain in red beets, like for the case of sugar, but the largest factor affecting composition was the plant's age. Therefore, for the first time, our results show that betalain can be used as a biomarker for plant age in red beet. This work demonstrates the power of Raman spectroscopy for the non-destructive and fast characterization of plants and their nutrients obtained in greenhouses at different developing times and under different conditions. These results demonstrate the spectroscopic tracking of a plant's component providing a new information tool for crops engineering and optimized farming.

Supplementary data to this article can be found online at https://doi.org/10.1016/j.saa.2019.01.006.

Acknowledgments

The work was carried out within the framework of the development program of the Project 5–100 National Research Tomsk Polytechnic University, Russia, Project VIU-OM-205/2018.

The authors declare no conflict of interest.

References

[1] P.M. Vitousek, R. Naylor, T. Crews, M.B. David, L.E. Drinkwater, E. Holland, P.J. Johnes, J. Katzenberger, L.A. Martinelli, P.A. Matson, G. Nziguheba, D. Ojima, C.A. Palm, G.P. Robertson, P.A. Sanchez, A.R. Townsend, F.S. Zhang, Nutrient imbalances in agricultural development, Science 324 (2009) 1519–1520, https://doi.org/10.1126/science.1170261.

[2] P.O. Lim, H.J. Kim, H.G. Nam, Leaf senescence, Annu. Rev. Plant Biol. 58 (2007) 115–136, https://doi.org/10.1146/annurev.arplant.57.032905.105316.

[3] H.-E. Khoo, K. Nagendra Prasad, K.-W. Kong, Y. Jiang, A. Ismail, Carotenoids and their isomers: color pigments in fruits and vegetables, Molecules 16 (2011) 1710–1738, https://doi.org/10.3390/molecules16021710.

[4] H.A. Bashir, A.-B.A. Abu-Goukh, Compositional changes during guava fruit ripening, Food Chem. 80 (2003) 557–563, https://doi.org/10.1016/s0308-8146(02)00345-x.

[5] R. Baranski, M. Baranska, H. Schulz, Changes in carotenoid content and distribution in living plant tissue can be observed and mapped in situ using NIR-FT-Raman spectroscopy, Planta 222 (2005) 448–457, https://doi.org/10.1007/s00425-005-1566-9.

[6] M.S. Günthardt-Goerg, P. Vollenweider, Linking stress with macroscopic and microscopic leaf response in trees: new diagnostic perspectives, Environ. Pollut. 147 (2007) 467–488, https://doi.org/10.1016/j.envpol.2006.08.033.

[7] J.W. Allwood, R. Goodacre, An introduction to liquid chromatography-mass spectrometry instrumentation applied in plant metabolomic analyses, Phytochem. Anal. 21 (2010) 33–47, https://doi.org/10.1002/pca.1187.

[8] X. Pan, R. Welti, X. Wang, Quantitative analysis of major plant hormones in crude plant extracts by high-performance liquid chromatography–mass spectrometry, Nat. Protoc. 5 (2010) 986, https://doi.org/10.1038/nprot.2010.37.

[9] C. Bicchi, S. Drigo, P. Rubiolo, Influence of fibre coating in headspace solid-phase microextraction–gas chromatographic analysis of aromatic and medicinal plants, J. Chromatogr. A 892 (2000) 469–485, https://doi.org/10.1016/s0021-9673(00)00231-4.

[10] M.E. Latorre, P. Narvaiz, A.M. Rojas, L.N. Gerschenson, Effects of gamma irradiation on bio-chemical and physico-chemical parameters of fresh-cut red beet (*Beta vulgaris* L. var. *conditiva*) root, J. Food Eng. 98 (2010) 178–191, https://doi.org/10.1016/j.jfoodeng.2009.12.024.

[11] Z. Basati, B. Jamshidi, M. Rasekh, Y. Abbaspour-Gilandeh, Detection of sunn pest-damaged wheat samples using visible/near-infrared spectroscopy based on pattern recognition, Spectrochim. Acta A Mol. Biomol. Spectrosc. 203 (2018) 308–314, https://doi.org/10.1016/j.saa.2018.05.123.

[12] C.S. Mangolim, C. Moriwaki, A.C. Nogueira, F. Sato, M.L. Baesso, A.M. Neto, G. Matioli, Curcumin-β-cyclodextrin inclusion complex: stability, solubility, characterisation by FT-IR, FT-Raman, X-ray diffraction and photoacoustic spectroscopy, and food application, Food Chem. 153 (2014) 361–370, https://doi.org/10.1016/j.foodchem.2013.12.067.

[13] N. Gierlinger, M. Schwanninger, The potential of Raman microscopy and Raman imaging in plant research, Spectroscopy 21 (2007) 69–89, https://doi.org/10.1155/2007/498206.

[14] J. Jehlička, P. Vitek, H.G.M. Edwards, M.D. Hargreaves, T. Čapoun, Fast detection of sulphate minerals (gypsum, anglesite, baryte) by a portable Raman spectrometer, J. Raman Spectrosc. 40 (2009) 1082–1086https://onlinelibrary.wiley.com/doi/abs/10.1002/jrs.2246.

[15] D. Lauwers, A.G. Hutado, V. Tanevska, L. Moens, D. Bersani, P. Vandenabeele, Characterisation of a portable Raman spectrometer for in situ analysis of art objects, Spectrochim. Acta A Mol. Biomol. Spectrosc. 118 (2014) 294–301, https://doi.org/10.1016/j.saa.2013.08.088.

[16] M. Gnyba, J. Smulko, A. Kwiatkowski, Portable Raman spectrometer-design rules and applications, Bull. Pol. 59 (2011) 325–329https://www.degruyter.com/view/j/bpasts.2011.59.issue-3/v10175-011-0040-z/v10175-011-0040-z.xml.

[17] H. Schulz, M. Baranska, Identification and quantification of valuable plant substances by IR and Raman spectroscopy, Vib. Spectrosc. 43 (2007) 13–25, https://doi.org/10.1016/j.vibspec.2006.06.001.

[18] S.J. Eichhorn, A. Dufresne, M. Aranguren, N.E. Marcovich, J.R. Capadona, S.J. Rowan, C. Weder, W. Thielemans, M. Roman, S. Renneckar, W. Gindl, S. Veigel, J. Keckes, H. Yano, K. Abe, M. Nogi, A.N. Nakagaito, A. Mangalam, J. Simonsen, A.S. Benight, A. Bismarck, L.A. Berglund, T. Peijs, Review: current international research into cellulose nanofibres and nanocomposites, J. Mater. Sci. 45 (1) (2009)https://doi.org/10.1007/s10853-009-3874-0.

[19] D. Klemm, B. Heublein, H.-P. Fink, A. Bohn, Cellulose: fascinating biopolymer and sustainable raw material, ChemInform 36 (2005)https://doi.org/10.1002/chin.200536238.

[20] S. Fischer, K. Schenzel, K. Fischer, W. Diepenbrock, Applications of FT Raman spectroscopy and micro spectroscopy characterizing cellulose and cellulosic biomaterials, Macromol. Symp. 223 (2005) 41–56, https://doi.org/10.1002/masy.200550503.

[21] M.F. Rosa, E.S. Medeiros, J.A. Malmonge, K.S. Gregorski, D.F. Wood, L.H.C. Mattoso, G. Glenn, W.J. Orts, S.H. Imam, Cellulose nanowhiskers from coconut husk fibers: effect of preparation conditions on their thermal and morphological behavior, Carbohydr. Polym. 81 (2010) 83–92, https://doi.org/10.1016/j.carbpol.2010.01.059.

[22] M. Szymańska-Chargot, J. Cybulska, A. Zdunek, Sensing the structural differences in cellulose from apple and bacterial cell wall materials by Raman and FT-IR spectroscopy, Sensors 11 (2011) 5543–5560, https://doi.org/10.3390/s110605543.

[23] R.M. El-Abassy, P. Donfack, A. Materny, Visible Raman spectroscopy for the discrimination of olive oils from different vegetable oils and the detection of adulteration, J. Raman Spectrosc. 40 (2009) 1284–1289, https://doi.org/10.1002/jrs.2279.

[24] A. Gliszczyńska-Świgło, H. Szymusiak, P. Malinowska, Betanin, the main pigment of red beet: molecular origin of its exceptionally high free radical-scavenging activity, Food Addit. Contam. 23 (2006) 1079–1087, https://doi.org/10.1080/02652030600986032.

[25] M. Maitah, L. Smutka, Restoration and growth of the Russian sugar market, Sugar Tech. 18 (2015) 115–123, https://doi.org/10.1007/s12355-015-0383-0.

[26] P. Ninfali, D. Angelino, Nutritional and functional potential of *Beta vulgaris* cicla and rubra, Fitoterapia 89 (2013) 188–199, https://doi.org/10.1016/j.fitote.2013.06.004.

[27] M. Bavec, M. Turinek, S. Grobelnik-Mlakar, A. Slatnar, F. Bavec, Influence of industrial and alternative farming systems on contents of sugars, organic acids, total phenolic content, and the antioxidant activity of red beet (*Beta vulgaris* L. ssp. *vulgaris* Rote Kugel), J. Agric. Food Chem. 58 (2010) 11825–11831, https://doi.org/10.1021/jf103085p.

[28] J. Escribano, J. Cabanes, M. Jiménez-Atiénzar, M. Ibañez-Tremolada, L.R. Gómez-Pando, F. García-Carmona, F. Gandía-Herrero, Characterization of betalains, saponins and antioxidant power in differently colored quinoa (*Chenopodium quinoa*) varieties, Food Chem. 234 (2017) 285–294, https://doi.org/10.1016/j.foodchem.2017.04.187.

[29] M. Olle, A. Viršile, The effects of light-emitting diode lighting on greenhouse plant growth and quality, Agric. Food Sci. 22 (2013) 223–234, https://doi.org/10.23986/afsci.7897.

[30] A. Pavlov, V. Georgiev, M. Ilieva, Betalain biosynthesis by red beet (*Beta vulgaris* L.) hairy root culture, Process Biochem. 40 (2005) 1531–1533, https://doi.org/10.1016/j.procbio.2004.01.001.

[31] N. Bhagyalakshmi, R. Thimmaraju, M.S. Narayan, Various hexoses and di-hexoses differently influence growth, morphology and pigment synthesis in transformed root cultures of red beet (*Beta vulgaris*), Plant Cell Tissue Organ Cult. 78 (2004) 183–195, https://doi.org/10.1023/b:ticu.0000022557.84867.db.

[32] F. Stagnari, A. Galieni, G. Cafiero, M. Pisante, Application of photo-selective films to manipulate wavelength of transmitted radiation and photosynthate composition in red beet (*Beta vulgaris* var. *conditiva* Alef.), J. Sci. Food Agric. 94 (2014) 713–720, https://doi.org/10.1002/jsfa.6312.

[33] B.-R. Lee, K.-Y. Kim, W.-J. Jung, J.-C. Avice, A. Ourry, T.-H. Kim, Peroxidases and lignification in relation to the intensity of water-deficit stress in white clover (*Trifolium repens* L.), J. Exp. Bot. 58 (2007) 1271–1279, https://doi.org/10.1093/jxb/erl280.

[34] V.E. de Oliveira, H.V. Castro, H.G.M. Edwards, L.F.C. de Oliveira, Carotenes and carotenoids in natural biological samples: a Raman spectroscopic analysis, J. Raman Spectrosc. 41 (2009) 642–650, https://doi.org/10.1002/jrs.2493.

[35] C. Sandquist, J.L. McHale, Improved efficiency of betanin-based dye-sensitized solar cells, J. Photochem. Photobiol. A Chem. 221 (2011) 90–97, https://doi.org/10.1016/j.jphotochem.2011.04.030.

[36] I. Belhadj Slimen, T. Najar, M. Abderrabba, Chemical and antioxidant properties of betalains, J. Agric. Food Chem. 65 (2017) 675–689, https://doi.org/10.1021/acs.jafc.6b04208.

[37] D.M. Marmion, Handbook of U.S. Colorants: Foods, Drugs, Cosmetics, and Medical Devices, John Wiley & Sons, 1991https://market.android.com/details?id=book-73NopCBKRsoC.

[38] G. Socrates, Infrared and Raman Characteristic Group Frequencies: Tables and Charts, John Wiley & Sons, 2004https://market.android.com/details?id=book-LDoAAjMnwEIC.

[39] M. Karabacak, Z. Calisir, M. Kurt, E. Kose, A. Atac, The spectroscopic (FT-IR, FT-Raman, dispersive Raman and NMR) study of ethyl-6-chloronicotinate molecule by combined density functional theory, Spectrochim. Acta A Mol. Biomol. Spectrosc. 153 (2016) 754–770, https://doi.org/10.1016/j.saa.2015.09.007.

[40] C. Qin, A.E. Clark, DFT characterization of the optical and redox properties of natural pigments relevant to dye-sensitized solar cells, Chem. Phys. Lett. 438 (2007) 26–30, https://doi.org/10.1016/j.cplett.2007.02.063.

[41] J. De Gelder, K. De Gussem, P. Vandenabeele, L. Moens, Reference database of Raman spectra of biological molecules, J. Raman Spectrosc. 38 (2007) 1133–1147, https://doi.org/10.1002/jrs.1734.

[42] J.V. Rau, V. Graziani, M. Fosca, C. Taffon, M. Rocchia, P. Crucitti, P. Pozzilli, A. Onetti Muda, M. Caricato, A. Crescenzi, RAMAN spectroscopy imaging improves the diagnosis of papillary thyroid carcinoma, Sci. Rep. 6 (2016), 35117. https://doi.org/10.1038/srep35117.

[43] R.B. Austin, Diurnal changes in the sugar and organic anion concentrations in red beet leaves, Ann. Bot. 36 (1972) 475–783, https://doi.org/10.1093/oxfordjournals.aob.a084606.